JOC The Journal of Organic Chemistry

Article

pubs.acs.org/joc

Regiochemical Effects of Furan Substitution on the Electronic Properties and Solid-State Structure of Partial Fused-Ring Oligothiophenes

John T. Henssler and Adam J. Matzger*

Department of Chemistry and the Macromolecular Science and Engineering Program, University of Michigan, 930 North University Avenue, Ann Arbor, Michigan 48109-1055, United States

Supporting Information

ABSTRACT: Oligomers containing the new fused-ring heterocyclic conjugated building block thieno[3,2-*b*]furan were synthesized, and the effects associated with furan ring substitution into fused-ring oligothiophenes on the electronic properties and solid-state structure were assessed. A series of four-ring oligomers which vary in the degree of furan ring substitution and the regiochemistry of placement were synthesized via Stille cross-coupling and oxidative homocoupling strategies. The electronic properties of these oligomers were studied by UV−vis absorption and fluorescence spectroscopies. Substitution of furan rings at the terminal positions yields oligomers with a narrower HOMO−LUMO gap relative to the all-thiophene analogue 2,2′-bithieno[3,2-*b*]thiophene, and incorporation of furan rings at the interior positions results in oligomers with an increase in rigidity and a higher fluorescence quantum yield. Packing motifs of the oligomers were determined using single crystal X-ray diffraction. In contrast to the herringbone crystal packing observed for nonfused oligothiophenes, oligofurans, thiophene−furan hybrid oligomers, and the all-thiophene analogue 2,2′-bithieno[3,2-*b*]thiophene, all three regioisomers derived from the dimerization of thieno[3,2-*b*]furan arrange in a π-stacked packing motif in the solid state.

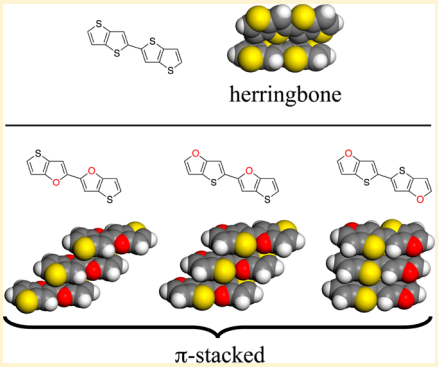

INTRODUCTION

Tailoring the electronic and solid-state properties of oligothiophenes through structural modification has been an area of intense research activity in recent years primarily due to potential applications in the field of organic electronics.[1−3] One general strategy that has received substantial attention is the replacement of a thiophene ring in α-oligothiophenes with another five-membered heteroaromatic moiety such as furan,[4−12] pyrrole,[10,13−16] silole,[17−20] and phosphole.[21−25] Thiophene−furan hybrid oligomers have displayed some more desirable properties than the pure oligothiophene analogues. For example, replacement of sulfur with oxygen tends to reduce spin−orbit coupling and thus decreases intersystem crossing, resulting in higher fluorescence quantum yields.[8,26] Furthermore, oxygen, which has a smaller van der Waals radius than sulfur, is credited with thiophene−furan hybrid oligomers achieving more densely packed herringbone arrangements as compared to the corresponding oligothiophene.[5,7] Altering the degree and regiochemistry of ring fusion are also effective methods of manipulating the electronic and solid-state properties of oligothiophenes.[27−29] For example, nonfused oligothiophenes assume a herringbone packing motif in the solid state; upon introduction of ring fusion, some oligothiophenes have been shown to adopt a π-stacked arrangement.[28,30] This change in packing motif is primarily attributed to the elimination of two β-hydrogen atoms for each degree of ring fusion (Figure 1) which reduces the number of potential electrostatic interactions between the hydrogen-dominated edges and the face (π-system) of adjacent molecules.[28,31,32] The π-stacked packing motif is predicted to be more favorable for charge carrier mobility due to the increase in π-orbital overlap.[33] Despite substantial interest, the number of thiophene-based oligomers that display π-stacking remains low, motivating our discovery of molecular design strategies that favor π-stacking of conjugated oligomers.

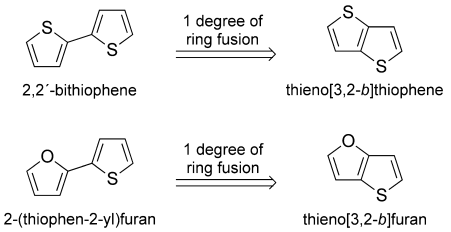

Figure 1. Structural comparison between nonfused α-linked and fused-ring heterocycles involving thiophene and furan.

The properties of nonfused thiophene−furan hybrid oligomers have been reported for systems that vary in the ratio of thiophene and furan rings,[4−12] but the effects of regiochemistry on the electronic properties and solid-state

Received: September 3, 2012
Published: September 17, 2012

Scheme 1. Synthetic Route to Oligomers 1−5[a]

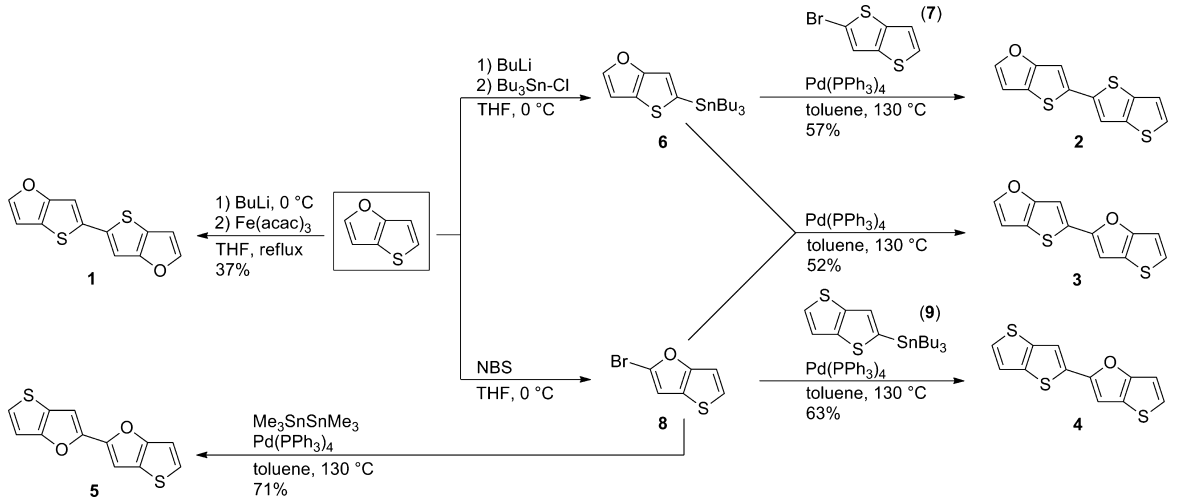

[a]Yields represent the material isolated by column chromatography in >96% purity (<4% regioisomers).

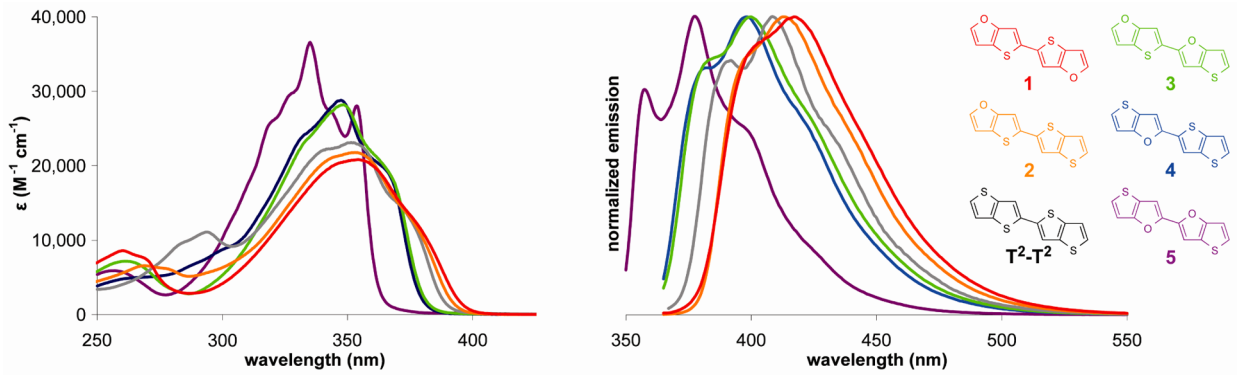

Figure 2. UV−vis absorption and emission spectra for oligomers **1**−**5** and T^2-T^2 in CH_2Cl_2.

packing have not been systematically evaluated. Further, until recently it was not possible to study the effect of ring fusion in alternating thiophene−furan hybrid systems due to the inaccessibility of the thiophene−furan fused-ring moiety thieno[3,2-*b*]furan.[34] In this investigation we utilized thieno-[3,2-*b*]furan and thieno[3,2-*b*]thiophene to generate a series of five four-ring oligomers in order to explore the effects of the extent of furan ring substitution and the regiochemistry of furan placement into the partial fused-ring oligothiophene 2,2′-bithieno[3,2-*b*]thiophene (T^2-T^2) on the electronic properties and solid-state packing arrangement. Specifically, all three regioisomers of the thieno[3,2-*b*]furan dimer were synthesized along with both regioisomers derived from the coupling of thieno[3,2-*b*]furan and thieno[3,2-*b*]thiophene moieties.

RESULTS AND DISCUSSION

Oligomer Synthesis. Oligomers **1**−**5** can be generated from thieno[3,2-*b*]furan[34] and thieno[3,2-*b*]thiophene[34] in two or fewer linear steps (Scheme 1). Oligomer **1** is derived directly from thieno[3,2-*b*]furan upon treatment with 1 equiv of butyllithium to generate the anion at the 5-position, followed by oxidative homocoupling employing $Fe(acac)_3$. The syntheses of oligomers **2**−**5** utilize tributyl(thieno[3,2-*b*]-furan-5-yl)stannane (**6**) and/or 2-bromothieno[3,2-*b*]furan (**8**) which are derived from thieno[3,2-*b*]furan in one step.[34] Intermediate **6** is coupled with 2-bromothieno[3,2-*b*]thiophene (**7**)[35] or **8** under Stille conditions to generate oligomers **2** and **3**, respectively. Intermediate **8** is cross-coupled with tributyl-(thieno[3,2-*b*]thiophene-5-yl)stannane (**9**)[36] or homocoupled under Stille type conditions to generate oligomers **4** and **5**, respectively.

Electronic Properties. The electronic properties of **1**−**5** were studies using UV−vis absorption and fluorescence spectroscopies (Figure 2). These data are compared to T^2-T^2 because it is the all-thiophene analogue of the oligomers under investigation and has been extensively studied.[28,29] Oligomers **1** and **2**, with furan rings at the periphery, yield a bathochromic shift of the absorption spectrum compared to that of T^2-T^2, indicating a narrower HOMO−LUMO gap. On the other hand, **4** and **5**, which contain furan rings at the interior of the structure, display a blue shift in the absorption spectrum relative to that of T^2-T^2, which reflects the reduced electron delocalization known to occur across furan rings.[26] Oligomer **3**, which consists of two thieno[3,2-*b*]furan units linked in a head-to-tail fashion and therefore is the only isomer with both an interior and exterior furan ring, yields a small blue shift in the absorption spectrum compared to T^2-T^2. The direction and relative magnitudes of these shifts indicate that placement of a furan ring at the terminal position acts to narrow the HOMO−LUMO gap, and positioning a furan ring at the interior of the molecule widens the optical band gap to a similar extent. For nonfused thiophene−furan hybrid oligomers, the effect of

dx.doi.org/10.1021/jo301744s | J. Org. Chem. 2012, 77, 9298−9303

regiochemistry on the position of the absorption envelope has not been previously evaluated but a compilation of the limited reports on such systems reveals that shifts in the longest wavelength absorption maximum (λ_{max}) values are similar to those observed for the partial fused-ring oligomers in this study.[8,9,29]

Inspection of the absorption profiles reveals information about the oligomer conformations in solution.[27,29,37] In the planar conformation orbital overlap and conjugative stabilization are greatest but the heteroatoms can influence the ground-state oligomer conformations and in many systems contribute to an increase in the population of molecules with nonplanar geometries. For example, α-linked thiophene rings experience steric repulsion between the sulfur atom of one ring and a β-hydrogen atom of an adjacent ring. Consequently α-oligothiophenes typically display broad, unstructured absorption profiles which reflect the twisted conformations and rotational freedom between adjacent rings in the aromatic system. In this study **1**, **2**, and $\mathbf{T^2}$-$\mathbf{T^2}$, which have two thiophene rings at the interior of the oligomer, display the broadest and least structured absorption envelopes, suggesting a larger population of oligomers in nonplanar conformations in comparison to **3**–**5** (Figure 2). In contrast, **5**, which contains two furan rings at the interior of the oligomer, yields the narrowest absorption profile with significantly more vibronic structure than **1**-**4** and $\mathbf{T^2}$-$\mathbf{T^2}$, and these features reflect a more rigid structure in solution (Figure 2). The higher degree of conformational rigidity for **5** can be attributed to replacement of sulfur with oxygen, having a smaller van der Waals radius, thus circumventing the issue of steric repulsion between adjacent rings.[38] Instead attractive intramolecular interactions between the oxygen of each interior furan ring and the β-hydrogen atom of the adjacent interior furan rings may contribute to the stabilization of the planar conformation.[39] Oligomers **3** and **4** each contain one thiophene and one furan ring at the central positions and show an intermediate broadening of the absorption profile (Figures 2). Trends associated with both the dihedral angle of the energy-minimized structure and the energy barrier of rotation between thiophene–thiophene, thiophene–furan, and furan–furan rings have been computationally investigated and are in accord with the assessment of the experimental absorption profiles above.[38−42] Further, extinction coefficients (ε) provide experimental evidence regarding oligomer conformation in the ground state. An increase in the extinction coefficient is expected as the conformation of an oligomer becomes more planar.[37,43] Indeed, a trend of increasing extinction coefficient from **1** to **5** is observed, coinciding with the above conformational assessment based on the shape of the absorption envelope.

The fluorescence λ_{max} values span 39 nm across the series of oligomers (Table 1), and comparison with the absorption λ_{max} values (the Stokes shift) also provides insight into molecular conformation in solution. Smaller Stokes shifts tend to be associated with molecules that undergo little change in conformation between the ground and the excited state, for example those which possess more rigid structures.[27,29,37] In agreement with the absorption profile analysis, **5** displays the smallest Stokes shift (Table 1), thus supporting the notion that it is the most rigid molecule in the series of oligomers in solution. As the furan rings are migrated toward the periphery of the oligomer, the Stokes shift increases and **1** has the largest Stokes shift.

Table 1. Electronic Properties for Oligomers 1–5 and 2,2′-Bithieno[3,2-*b*]thiophene in CH_2Cl_2

oligomer		abs λ_{max} (nm)	ε_{max} (M^{-1} cm^{-1})	em λ_{max} (nm)	Stokes shift (nm)	Φ_f (%)
1	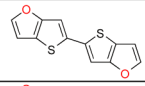	355	20,800	417	62	30
2	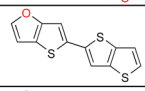	353	21,700	413	60	15
$\mathbf{T^2}$-$\mathbf{T^2}$	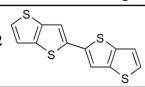	351	23,100	410	59	18
3	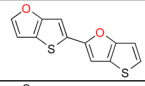	349	28,200	400	51	38
4	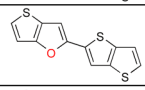	347	28,800	397	50	44
5	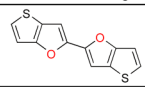	335	36,700	378	43	93

Oligomers **1**, **3**, **4**, and **5** exhibit higher fluorescence quantum yields (Φ_F) as compared to $\mathbf{T^2}$-$\mathbf{T^2}$ (Table 1). Most notably, **5** displays a 5-fold increase in the fluorescence quantum yield. This result may be attributed to both increased planarization and reduced influence of the heavy atom effect.[26,44,45] Introduction of furan rings into oligothiophenes typically results in an increase in the fluorescence quantum yield but in a very small number of cases, when furan rings are located in noncentral positions of the molecule, a decrease in emission efficiency has been observed.[8] Likewise, **2** displays a fluorescence quantum yield slightly lower than that of $\mathbf{T^2}$-$\mathbf{T^2}$. Despite reports aimed specifically at determining the cause of photophysical phenomena such as reduced fluorescence quantum yield in some thiophene–furan hybrid oligomers, the explanation remains elusive.[8,26]

Solid-State Structure. The single crystal structures of **1**, **3**, and **5** were determined to elucidate the role of intermolecular interactions in the solid-state packing arrangements in this series of thieno[3,2-*b*]furan dimers. The significant difference between the propensity of **1**, **3**, and **5** versus the all-thiophene analogue $\mathbf{T^2}$-$\mathbf{T^2}$ to form single crystals larger than 0.03 mm × 0.03 mm × 0.01 mm should be noted. In comparison to oligothiophenes, the thieno[3,2-*b*]furan dimers form significantly larger single crystals (>0.5 mm × 0.3 mm × 0.1 mm by slow evaporation from organic solvents). These observations suggest that the thieno[3,2-*b*]furan moiety acts to enhance solid-state ordering over longer distances in comparison to thieno[3,2-*b*]thiophene.

Oligomer **5** displays a slipped π-stacked arrangement with a face-to-face intermolecular distance of 3.49 Å (Figure 3). The distance between π-stacked oligomers was determined by a perpendicular measurement between a plane defined by one five-membered ring and the centroid of an overlapping five-membered ring in an adjacent face-to-face oriented molecule. The oligomer exists in a planar transoid conformation, and short intramolecular C_β–H···O distances (2.88 Å) are observed. Both internal furan rings present close intermolecular C_β–H···O contacts (2.45 Å) between furan rings in neighboring molecules. The α-hydrogen on each of the

dx.doi.org/10.1021/jo301744s | J. Org. Chem. 2012, 77, 9298–9303

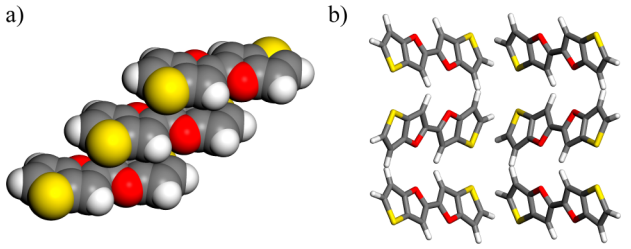

Figure 3. Crystal structure diagram of oligomer **5** illustrating (a) the slipped π-stacked packing motif and (b) the orientation of oligomers in adjacent columns.

terminal thiophene rings forms close interactions with the thienyl sulfur and π-system (2.72 and 2.73 Å, respectively) of the terminal thiophene ring in a molecule adjacent to the short edge of the oligomer.

The structure of **3** reveals a slipped π-stacked motif with a close face-to-face intermolecular distance of 3.33 Å, and the oligomer exists in the cisoid conformation with a torsion angle of 3° (Figure 4). The sulfur and oxygen in the central rings are

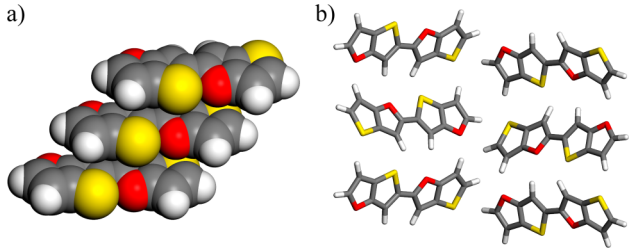

Figure 4. Crystal structure diagram of oligomer **3** illustrating (a) the slipped π-stacked packing motif and (b) the orientation of oligomers in adjacent columns.

observed at a distance of 2.94 Å, which is considerably shorter than the sum of the van der Waals radii for the two atoms (3.32 Å). A close C_β–H···S interaction (2.87 Å) is present between the internal furan and thiophene rings of molecules in neighboring columns. Short C_β–H···S and C_β–H···O distances (2.92 and 2.49 Å, respectively) are found between terminal thiophene and furan rings in molecules that adjoin the long edge of the structure. Oligomers also interact along the short edge of the structure; the terminal thiophene ring forms a close C_α–H···O contact (2.50 Å) with a terminal furan ring, which displays close C_α–H···S and C_α–H···π interactions (2.80 and 2.68 Å, respectively) with a terminal thiophene ring in another molecule adjacent to the short edge of the oligomer.

Oligomer **1** adopts a slipped π-stacked motif with a short face-to-face intermolecular distance of 3.45 Å (Figure 5). Like

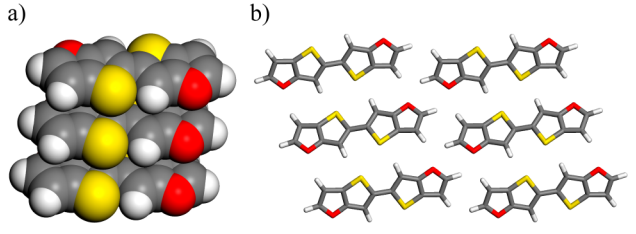

Figure 5. Crystal structure diagram of oligomer **1** illustrating (a) the slipped π-stacked packing motif and (b) the orientation of oligomers in adjacent columns.

5, oligomer **1** arranges in a planar transoid fashion. Both internal thiophene rings exhibit short C_β–H···S contacts (2.89 Å) with thiophene rings in adjacent oligomers. Close C_α–H···O (2.55 Å) and C_β–H···O (2.50 Å) interactions are present between the terminal furan rings of molecules in neighboring columns.

The solid-state packing arrangements of **1**, **3**, and **5** all display π–π interactions, which are markedly different from the herringbone motif adopted by the oligothiophene analogue $\mathbf{T^2}$-$\mathbf{T^2}$ (Figure 6).[28] Furthermore, nonfused oligothiophenes,[46−53]

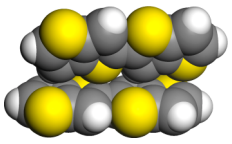

Figure 6. Crystal structure diagram of $\mathbf{T^2}$-$\mathbf{T^2}$ illustrating the herringbone packing motif.[28]

oligofurans,[40] and thiophene–furan hybrid oligomers[5,7] arrange in a herringbone fashion; neither adjusting the ratio of furan and thiophene rings or the partial ring fusion in $\mathbf{T^2}$-$\mathbf{T^2}$ has been demonstrated to yield oligomers with π-stacked packing arrangements. The packing motifs of **1**, **3**, and **5** may be attributed to a combination of the following features, which are unique to these oligomers. First, the furan rings facilitate the formation of an extensive network of intermolecular C–H···O interactions as previously discussed. These interactions occur at distances which are considerably closer than the sum of the van der Waals radii for O and H (2.61 Å). Second, the condensed ring approach eliminates β-hydrogen atoms, thereby increasing the C/H ratio and favoring π–π interactions in the solid state.[28] Notably, no close interactions exist between β-hydrogen atoms and the π-system of neighboring molecules in the crystal structures of **1**, **3**, or **5**. Instead, short intermolecular C_β–H···O interactions are prevalent.

Substitution of furan into nonfused oligothiophenes has been reported to result in more densely packed herringbone structures.[5,7] A direct comparison cannot be made among **1**, **3**, and **5** versus $\mathbf{T^2}$-$\mathbf{T^2}$ due to the distinct difference in packing motifs. Instead, pentathienoacene is the most appropriate comparison compound because, like **1**, **3**, and **5**, it also contains six double bonds and presents a π-stacked arrangement in the solid state. All three thieno[3,2-*b*]furan dimers display shorter π-stacked distances (3.33–3.49 Å) than the reported value for pentathienoacene (3.52 Å),[54] which may be attributed to the smaller van der Walls radius of oxygen in comparison to sulfur. For example, **3** exhibits S···O contact between π-stacked oligomers at a distance of 3.38 Å, which is shorter than those observed for short S···S contacts.

■ CONCLUSION

In summary, a series of oligomers containing the fused-ring unit thieno[3,2-*b*]furan were synthesized. It was found that migration of the furan ring toward the terminal position of the oligomer results in a narrowing of the HOMO–LUMO gap, whereas placement of furan at the interior position yields an increase in planarization, extinction coefficient, and fluorescence quantum yield in solution. In the solid state, all three regioisomer dimers of thieno[3,2-*b*]furan present π–π interactions which are absent in nonfused oligothiophenes, oligofurans, thiophene–furan hybrid oligomers, and the

dx.doi.org/10.1021/jo301744s | J. Org. Chem. 2012, 77, 9298–9303

thiophene analogue 2,2′-bithieno[3,2-*b*]thiophene. Therefore, the combination of ring fusion and furan incorporation into oligothiophenes serves as a new approach to engineer the electronic and solid-state properties of conjugated materials.

EXPERIMENTAL SECTION

General. Thieno[3,2-*b*]furan,[34] 2-bromothieno[3,2-*b*]furan,[34] tributyl(thieno[3,2-*b*]furan-5-yl)stannane,[34] 2-bromothieno[3,2-*b*]-thiophene,[35] and tributyl(thieno[3,2-*b*]thiophen-2-yl)stannane[36] were prepared according to literature procedures. 2-Bromothieno[3,2-*b*]furan and tributyl(thieno[3,2-*b*]furan-5-yl)stannane were each >96% pure, with the impurity being the regioisomers tributyl(thieno-[3,2-*b*]furan-2-yl)stannane and 5-bromothieno[3,2-*b*]furan, respectively.[34] THF was dried by passage through a column packed with activated alumina. UV−vis spectroscopy was performed in CH_2Cl_2 solution (>10^{-5} M) at room temperature. Emission spectra were collected in CH_2Cl_2 solution (>10^{-8} M) at room temperature, and samples were excited at the wavelength corresponding to the longest wavelength absorption maximum (Table 1). Infrared absorption spectra were collected on a FT-IR instrument. Melting point ranges were determined using a melting point apparatus equipped with a thermocouple. Crystals of **1**, **3**, and **5** suitable for single crystal X-ray diffraction were obtained by slow evaporation from a mixture of 3% CH_2Cl_2 and 97% hexanes.

5,5′-Bithieno[3,2-*b*]furan (1). In a dry two-neck flask fitted with a reflux condenser, thieno[3,2-*b*]furan (208 mg, 1.68 mmol) was dissolved in THF (30 mL), and the solution was sparged with N_2 gas. A 1.6 M butyllithium solution in hexanes (1.00 mL, 1.60 mmol) was added to the solution at 0 °C under a N_2 atmosphere. After 30 min at this temperature, the reaction mixture was allowed to warm to rt over 15 min. $Fe(acac)_3$ (1.13 g, 3.20 mmol) was then added to the flask in one portion, and the solution was heated to reflux for 12 h. Upon cooling to rt, the reaction mixture was poured into stirring ethanol and cooled to −78 °C. The resulting precipitate was collected by cold filtration on a fritted funnel and rinsed with cold ethanol. The crude solid was purified by column chromatography on silica gel (3% CH_2Cl_2 in hexanes) to yield **1** (73.0 mg, 37%) as the major product (>96% pure) with the impurity being the regioisomers. A portion of pure **1** was isolated for characterization. mp 137−138 °C. UV−vis (CH_2Cl_2): λ (log ε) = 370 (4.19, sh), 354 (4.32), 259 (3.93) nm. ^{1}H NMR (500 MHz, $CDCl_3$, δ): 7.53 (d, J = 2.1 Hz, 2H), 7.17 (d, J = 0.6 Hz, 2H), 6.73 (dd, J = 2.1, 0.6 Hz, 2H). ^{13}C NMR (125 MHz, $CDCl_3$, δ): 157.4, 145.7, 138.1, 122.2, 107.3, 106.2. IR (KBr): 3144 (vw), 3120 (w), 3070 (w), 1680 (vw), 1597 (w), 1479 (m), 1373 (m), 1336 (m), 1165 (w), 1132 (m), 1063 (m), 1003 (m), 897 (m), 847 (w), 795 (vs), 733 (s), 719 (vs), 675 (m), 577 (m), 552 (m) cm^{-1}. MS (EI, 70 eV) m/z (relative intensity): 249.0 (1.4), 248.0 (9.9), 247.0 (14.5), 246.0 (100, M$^+$), 217.0 (32.8), 189.9 (27.9), 185.0 (19.2), 69.0 (59.8). Anal. Calcd for $C_{12}H_6O_2S_2$: C, 58.52; H, 2.46. Found: C, 58.56; H, 2.32.

5-(Thieno[3,2-*b*]thiophen-2-yl)thieno[3,2-*b*]furan (2). In a pressure vessel, tributyl(thieno[3,2-*b*]furan-5-yl)stannane (**6**, 413 mg, 1.00 mmol) and 2-bromothieno[3,2-*b*]thiophene (**7**, 219 mg, 1.00 mmol) were combined in toluene (10 mL), and the solution was sparged with N_2 gas. $Pd(PPh_3)_4$ (23.1 mg, 20.0 μmol) was added to the mixture all at once, and the vessel was quickly sealed. The reaction mixture was stirred for 12 h at 130 °C. The solution was then diluted with hexanes and passed through a silica plug. Solvent was removed from the filtrate in vacuo, and the residue was recrystallized from methanol (−78 °C). The solid was collected by cold filtration on a fritted funnel, rinsed with cold methanol, and then purified by column chromatography on silica gel (3% CH_2Cl_2 in hexanes) to yield **2** (150 mg, 57%) as the major product (>96% pure) with the impurity being the regioisomers. A portion of pure **2** was isolated for characterization. mp 170−171 °C. UV−vis (CH_2Cl_2): λ (log ε) = 368 (4.20, sh), 353 (4.34), 345 (4.33, sh), 269 (3.83, sh) nm. ^{1}H NMR (500 MHz, $CDCl_3$, δ): 7.54 (d, J = 2.1 Hz, 1H), 7.37 (d, J = 0.6 Hz, 1H), 7.36 (d, J = 5.3 Hz, 1H), 7.23 (dd, J = 5.3, 0.6 Hz, 1H), 7.20 (d, J = 0.6 Hz, 1H), 6.73 (dd, J = 2.1, 0.6 Hz, 1H). ^{13}C NMR (125 MHz, $CDCl_3$, δ): 157.4, 145.8, 139.8, 139.7, 138.0, 137.6, 127.2, 122.4, 119.4, 115.4, 107.8, 106.2. IR (KBr): 3109 (w), 3074 (w), 2922 (vw), 2852 (vw), 1606 (w), 1502 (w), 1477 (w), 1454 (w), 1398 (w), 1348 (m), 1194 (w), 1160 (w), 1130 (w), 1055 (s), 1005 (w), 926 (w), 897 (m), 797 (vs), 764 (m), 743 (m), 733 (m), 723 (s), 702 (vs), 677 (m), 630 (m), 552 (m) cm^{-1}. MS (EI, 70 eV) m/z (relative intensity): 265.0 (2.0), 264.0 (14.4), 263.0 (15.8), 262.0 (100, M$^+$), 232.9 (57.3), 200.9 (32.7), 68.9 (54.2). Anal. Calcd for $C_{12}H_6OS_3$: C, 54.93; H, 2.31. Found: C, 55.08; H, 2.21.

2,5′-Bithieno[3,2-*b*]furan (3). The title compound was prepared according to a procedure analogous to that used for the synthesis of **2**, except using tributyl(thieno[3,2-*b*]furan-5-yl)stannane (**6**, 413 mg, 1.00 mmol), 2-bromothieno[3,2-*b*]furan (**8**, 203 mg, 1.00 mmol), and $Pd(PPh_3)_4$ (23.1 mg, 20.0 μmol) to yield **3** (130 mg, 52%) as the major product (>96% pure), with the impurity being the regioisomers. A portion of pure **3** was isolated for characterization. mp 114−115 °C. UV−vis (CH_2Cl_2): λ (log ε) = 360 (4.34, sh), 349 (4.45), 335 (4.38, sh), 261 (3.86) nm. ^{1}H NMR (500 MHz, $CDCl_3$, δ): 7.55 (d, J = 2.1 Hz, 1H), 7.31 (s, 1H), 7.18 (d, J = 5.3 Hz, 1H), 7.07 (dd, J = 5.3, 0.6 Hz, 1H), 6.86 (s, 1H), 6.75 (dd, J = 2.1, 0.6 Hz, 1H). ^{13}C NMR (125 MHz, $CDCl_3$, δ): 157.6, 157.2, 152.9, 146.0, 133.4, 125.5, 125.1, 122.5, 110.8, 106.7, 106.3, 100.9. IR (KBr): 3136 (w), 3111 (w), 3091 (w), 2953 (vw), 2922 (vw), 2850 (vw), 1560 (w), 1500 (w), 1479 (w), 1458 (w), 1410 (w), 1402 (w), 1352 (s), 1211 (w), 1130 (w), 1088 (w), 1059 (m), 1034 (w), 1005 (w), 972 (m), 895 (m), 862 (w), 804 (m), 785 (s), 733 (vs), 706 (vs), 681 (m), 656 (s), 646 (m), 554 (m), 521 (m) cm^{-1}. MS (EI, 70 eV) m/z (relative intensity): 249.0 (1.2), 248.0 (10.0), 247.0 (14.9), 246 (100, M$^+$), 217.0 (48.3), 192.0 (43.2), 148.0 (33.0), 95.1 (23.1), 93.0 (30.8), 82.1 (22.9), 69.0 (47.3). Anal. Calcd for $C_{12}H_6O_2S_2$: C, 58.52; H, 2.46. Found: C, 58.59; H, 2.28.

2-(Thieno[3,2-*b*]thiophen-2-yl)thieno[3,2-*b*]furan (4). The title compound was prepared according to a procedure analogous to that used for the synthesis of **2**, except using tributyl(thieno[3,2-*b*]thiophen-2-yl)stannane (**9**, 429 mg, 1.00 mmol), 2-bromothieno-[3,2-*b*]furan (**8**, 203 mg, 1.00 mmol), and $Pd(PPh_3)_4$ (23.1 mg, 20.0 μmol) to yield **4** (166 mg, 63%) as the major product (>96% pure), with the impurity being the regioisomers. A portion of pure **4** was isolated for characterization. mp 178−179 °C. UV−vis (CH_2Cl_2): λ (log ε) = 359 (4.33, sh), 347 (4.46), 335 (4.40, sh), 269 (3.70) nm. ^{1}H NMR (500 MHz, $CDCl_3$, δ): 7.51 (s, 1H), 7.38 (d, J = 5.2 Hz, 1H), 7.25 (dd, J = 5.2, 0.6 Hz, 1H), 7.20 (d, J = 5.3 Hz, 1H), 7.08 (dd, J = 5.3, 0.6 Hz, 1H), 6.89 (s, 1H). ^{13}C NMR (125 MHz, $CDCl_3$, δ): 157.4, 152.6, 139.8, 138.2, 135.2, 127.6, 125.6, 125.1, 119.5, 115.1, 110.8, 101.4. IR (KBr): 3126 (w), 3107 (w), 3078 (w), 2918 (vw), 2848 (vw), 1556 (w), 1502 (w), 1466 (w), 1452 (w), 1439 (m), 1414 (w), 1350 (m), 1215 (w), 1190 (w), 1157 (w), 1082 (w), 1036 (w), 989 (m), 918 (m), 814 (m), 787 (s), 739 (m), 700 (vs), 658 (m), 644 (s), 633 (m), 527 (m) cm^{-1}. MS (EI, 70 eV) m/z (relative intensity): 265.0 (2.1), 264.0 (14.2), 263.0 (16.5), 262.0 (100, M$^+$), 233.0 (41.2), 207.9 (51.1), 163.9 (44.7), 95.1 (25.6), 82.1 (28.6), 69.0 (39.3). Anal. Calcd for $C_{12}H_6OS_3$: C, 54.93; H, 2.31. Found: C, 54.97; H, 2.21.

2,2′-Bithieno[3,2-*b*]furan (5). The title compound was prepared according to a procedure analogous to that used for the synthesis of **2**, except using hexamethylditin (328 mg, 1.00 mmol), 2-bromothieno-[3,2-*b*]furan (**8**, 406 mg, 2.00 mmol), and $Pd(PPh_3)_4$ (23.1 mg, 20.0 μmol) to yield **5** (176 mg, 71%) as the major product (>96% pure) with the impurity being the regioisomers. A portion of pure **5** was isolated for characterization. mp 225−226 °C. UV−vis (CH_2Cl_2): λ (log ε) = 353 (4.45), 342 (4.44, sh), 335 (4.56), 328 (447, sh), 320 (4.42, sh), 225 (4.40) nm. ^{1}H NMR (500 MHz, $CDCl_3$, δ): 7.22 (d, J = 5.3 Hz, 1H), 7.09 (dd, J = 5.3, 0.5 Hz, 1H), 6.98 (d, J = 0.5 Hz, H). ^{13}C NMR (125 MHz, $CDCl_3$, δ): 157.6, 149.4, 126.0, 124.9, 110.8, 101.7. IR (KBr): 3134 (w), 3122 (w), 3107 (vw), 3093 (w), 1599 (w), 1444 (s), 1360 (w), 1178 (m), 1088 (m), 1043 (s), 1026 (s), 893 (s), 858 (s), 827 (m), 798 (vs), 735 (s), 704 (vs), 654 (vs), 548 (m) cm^{-1}. MS (EI, 70 eV) m/z (relative intensity): 249.1 (1.25), 248.1 (9.7), 247.1 (15.0), 246.1 (100, M$^+$), 217.1 (26.2), 192.0 (75.6), 148.0 (23.9), 69.0 (30.4). Anal. Calcd for $C_{12}H_6O_2S_2$: C, 58.52; H, 2.46. Found: C, 58.52; H, 2.43.

dx.doi.org/10.1021/jo301744s | J. Org. Chem. 2012, 77, 9298−9303

■ ASSOCIATED CONTENT

Supporting Information

Experimental procedures and NMR spectra for **1**−**5**, as well as CIF files and crystallographic information for **1**, **3**, and **5**. This material is available free of charge via the Internet at http://pubs.acs.org.

■ AUTHOR INFORMATION

Corresponding Author

*E-mail: matzger@umich.edu.

Notes

The authors declare no competing financial interest.

■ ACKNOWLEDGMENTS

This work was supported by the National Science Foundation (CHE 0957591). The authors thank Dr. William W. Porter III for X-ray structure determination.

■ REFERENCES

(1) Mishra, A.; Ma, C. Q.; Bäuerle, P. *Chem. Rev.* **2009**, *109*, 1141.
(2) Fukazawa, A.; Yamaguchi, S. *Chem. Asian J.* **2009**, *4*, 1386.
(3) Murphy, A. R.; Fréchet, J. M. J. *Chem. Rev.* **2007**, *107*, 1066.
(4) Bunz, U. H. F. *Angew. Chem., Int. Ed.* **2010**, *49*, 5037.
(5) Miyata, Y.; Terayama, M.; Minari, T.; Nishinaga, T.; Nemoto, T.; Isoda, S.; Komatsu, K. *Chem. Asian J.* **2007**, *2*, 1492.
(6) Minari, T.; Miyata, Y.; Terayama, M.; Nemoto, T.; Nishinaga, T.; Komatsu, K.; Isoda, S. *Appl. Phys. Lett.* **2006**, *88*, 033514.
(7) Miyata, Y.; Nishinaga, T.; Komatsu, K. *J. Org. Chem.* **2005**, *70*, 1147.
(8) de Melo, J. S.; Elisei, F.; Becker, R. S. *J. Chem. Phys.* **2002**, *117*, 4428.
(9) Hucke, A.; Cava, M. P. *J. Org. Chem.* **1998**, *63*, 7413.
(10) Parakka, J. P.; Cava, M. P. *Synth. Met.* **1995**, *68*, 275.
(11) Joshi, M. V.; Hemler, C.; Cava, M. P.; Cain, J. L.; Bakker, M. G.; McKinley, A. J.; Metzger, R. M. *J. Chem. Soc., Perk. Trans. 2* **1993**, 1081.
(12) Wynberg, H.; Sinnige, H. J. M.; Creemers, H. M. J. C. *J. Org. Chem.* **1971**, *36*, 1011.
(13) van Haare, J. A. E. H.; Groenendaal, L.; Peerlings, H. W. I.; Havinga, E. E.; Vekemans, J. A. J. M.; Janssen, R. A. J.; Meijer, E. W. *Chem. Mater.* **2002**, *7*, 1984.
(14) Kozaki, M.; Parakka, J. P.; Cava, M. P. *J. Org. Chem.* **1996**, *61*, 3657.
(15) Parakka, J. P.; Jeevarajan, J. A.; Jeevarajan, A. S.; Kispert, L. D.; Cava, M. P. *Adv. Mater.* **1996**, *8*, 54.
(16) Groenendaal, L.; Peerlings, H. W. I.; Havinga, E. E.; Vekemans, J. A. J. M.; Meijer, E. W. *Synth. Met.* **1995**, *69*, 467.
(17) Zhang, G.; Ma, J.; Jiang, Y. *Macromolecules* **2003**, *36*, 2130.
(18) Yamaguchi, S.; Goto, T.; Tamao, K. *Angew. Chem., Int. Ed.* **2000**, *39*, 1695.
(19) Tamao, K.; Uchida, M.; Izumizawa, T.; Furukawa, K.; Yamaguchi, S. *J. Am. Chem. Soc.* **1996**, *118*, 11974.
(20) Tamao, K.; Yamaguchi, S.; Ito, Y.; Matsuzaki, Y.; Yamabe, T.; Fukushima, M.; Mori, S. *Macromolecules* **1995**, *28*, 8668.
(21) Fave, C.; Cho, T.-Y.; Hissler, M.; Chen, C.-W.; Luh, T.-Y.; Wu, C.-C.; Réau, R. *J. Am. Chem. Soc.* **2003**, *125*, 9254.
(22) Hay, C.; Fave, C.; Hissler, M.; Rault-Berthelot, J.; Réau, R. *Org. Lett.* **2003**, *5*, 3467.
(23) Delaere, D.; Nguyen, M. T.; Vanquickenborne, L. G. *J. Phys. Chem. A* **2003**, *107*, 838.
(24) Hay, C.; Hissler, M.; Fischmeister, C.; Rault-Berthelot, J.; Toupet, L.; Nyulászi, L.; Réau, R. *Chem.—Eur. J.* **2001**, *7*, 4222.
(25) Hay, C.; Fischmeister, C.; Hissler, M.; Toupet, L.; Réau, R. *Angew. Chem., Int. Ed.* **2000**, *39*, 1812.
(26) de Melo, J. S.; Elisei, F.; Gartner, C.; Aloisi, G. G.; Becker, R. S. *J. Phys. Chem. A* **2000**, *104*, 6907.
(27) Henssler, J. T.; Zhang, X.; Matzger, A. J. *J. Org. Chem.* **2009**, *74*, 9112.
(28) Zhang, X.; Johnson, J. P.; Kampf, J. W.; Matzger, A. J. *Chem. Mater.* **2006**, *18*, 3470.
(29) Zhang, X.; Matzger, A. J. *J. Org. Chem.* **2003**, *68*, 9813.
(30) Li, X. C.; Sirringhaus, H.; Garnier, F.; Holmes, A. B.; Moratti, S. C.; Feeder, N.; Clegg, W.; Teat, S. J.; Friend, R. H. *J. Am. Chem. Soc.* **1998**, *120*, 2206.
(31) G. R. Desiraju, G. A. *Acta Crystallogr., Sect. B: Struct. Sci* **1989**, *45*, 473.
(32) Gavezzotti, A.; Desiraju, G. R. *Acta Crystallogr., Sect. B: Struct. Sci* **1988**, *44*, 427.
(33) Brédas, J. L.; Calbert, J. P.; da Silva, D. A.; Cornil, J. *Proc. Natl. Acad. Sci. U.S.A.* **2002**, *99*, 5804.
(34) Henssler, J. T.; Matzger, A. J. *Org. Lett.* **2009**, *11*, 3144.
(35) Bugge, A. *Acta Chem. Scand.* **1969**, *23*, 2704.
(36) Prim, D.; Kirsch, G. *J. Chem. Soc., Perkin Trans. 1* **1994**, 2603.
(37) Berlman, I. B. *J. Phys. Chem.* **1970**, *74*, 3085.
(38) Diaz-Quijada, G. A.; Weinberg, N.; Holdcroft, S.; Pinto, B. M. *J. Phys. Chem. A* **2002**, *106*, 1266.
(39) Balbás, A.; Tejera, M. J. G.; Tortajada, J. *THEOCHEM* **2001**, *572*, 141.
(40) Gidron, O.; Diskin-Posner, Y.; Bendikov, M. *J. Am. Chem. Soc.* **2010**, *132*, 2148.
(41) Zade, S. S.; Bendikov, M. *Chem.—Eur. J.* **2007**, *13*, 3688.
(42) Karpfen, A.; Choi, C. H.; Kertesz, M. *J. Phys. Chem. A* **1997**, *101*, 7426.
(43) Radke, K. R.; Ogawa, K.; Rasmussen, S. C. *Org. Lett.* **2005**, *7*, 5253.
(44) Ohulchanskyy, T. Y.; Donnelly, D. J.; Detty, M. R.; Prasad, P. N. *J. Phys. Chem. B* **2004**, *108*, 8668.
(45) Mitschke, U.; Osteritz, E. M.; Debaerdemaeker, T.; Sokolowski, M.; Bäuerle, P. *Chem.—Eur. J.* **1998**, *4*, 2211.
(46) Facchetti, A.; Yoon, M. H.; Stern, C. L.; Hutchison, G. R.; Ratner, M. A.; Marks, T. J. *J. Am. Chem. Soc.* **2004**, *126*, 13480.
(47) Azumi, R.; Goto, M.; Honda, K.; Matsumoto, M. *Bull. Chem. Soc. Jpn.* **2003**, *76*, 1561.
(48) Cornil, J.; Beljonne, D.; Calbert, J. P.; Brédas, J. L. *Adv. Mater.* **2001**, *13*, 1053.
(49) Antolini, L.; Horowitz, G.; Kouki, F.; Garnier, F. *Adv. Mater.* **1998**, *10*, 382.
(50) Siegrist, T.; Kloc, C.; Laudise, R. A.; Katz, H. E.; Haddon, R. C. *Adv. Mater.* **1998**, *10*, 379.
(51) Kloc, C.; Simpkins, P. G.; Siegrist, T.; Laudise, R. A. *J. Cryst. Growth* **1997**, *182*, 416.
(52) Horowitz, G.; Bachet, B.; Yassar, A.; Lang, P.; Demanze, F.; Fave, J.-L.; Garnier, F. *Chem. Mater.* **1995**, *7*, 1337.
(53) Hotta, S.; Waragai, K. *J. Mater. Chem.* **1991**, *1*, 835.
(54) Zhang, X.; Côté, A. P.; Matzger, A. J. *J. Am. Chem. Soc.* **2005**, *127*, 10502.